A recognition of filaments in solar images with an Artificial Neural Network

V.V.Zharkova[1] and V.Schetinin [2]

[1]Cybernetics Department, Bradford University, UK:V.V.Zharkova@brad.ac.uk.
[2]Computer Science Department , Exeter University, UK: V.Schetinin@ex.ac.uk

Abstract. A new technique based on the Artificial Neural Network (ANN) was developed for an automated recognition of solar filaments, dark elongated features visible in the hydrogen Halpha line full disk spectroheliograms. The ANN was trained on a single fragment containing the filament elements depicted on a local background and then tested on the other 54 image fragments depicting filaments on the backgrounds with variations in brightness. Despite the difference in backgrounds, the ANN has properly recognized filaments in all the testing image fragments. This technique can be extended for an automated recognition of solar filaments in the existing solar catalogues.

1. Introduction

Solar images observed from the ground and space-based observatories in various wavelengths were digitized and stored in different catalogues. There is a growing interest to automate processing of a bulk of the ground-based full disk Hydrogen H_α-line observations [1], which can provide important information on the long-term solar activity variations during months or years. The project European Grid of Solar Observations [2] was designed to deal with the automated detection of various features associated with solar activity, such as: sunspots, active regions and filaments, solar prominences and others.

Filaments are the projections on a solar disk of prominences seen as very bright and large-scale features on the solar limb [1]. Their location and shape does not change very much for a long time and, hence, their lifetime is likely to be much longer then one solar rotation. However, there are visible changes seen in the filament elongation, position with respect to an active region and magnetic field configuration. For this reason the automated detection of solar filaments is a very important task to tackle in sense of understanding the physics of prominence formation, support and disruptions. Quite a few techniques were explored for a different level of the feature detection such as: the rough detection with a mosaic threshold technique [3], image segmentation and region growing techniques [4].

Artificial Neural Networks (ANNs) methods [5, 6], which were applied to the filament recognition problem, normally require a representative set of image data available for training. The training data have to represent the image fragments, depicting filaments on different conditions, under which the ANN has to solve the recognition problem and, for this reason, a number of the training examples has to be rather big. The paper presents the ANN technique learning the rules for filament recognition

from a single image fragment, which was labeled manually. This technique has been successfully tested on many other filament fragments and, potentially, can be extended for an automated recognition of filaments from a full disk solar image.

2. A Problem Definition

Let us introduce a $n \times m$ matrix $\mathbf{X} = \{x_{ij}\}$, $i = 1, \ldots, n$, $j = 1, \ldots, m$, consisting of the pixels whose brightness ranges between 1 and 255: $x_{ij} \in (1, 255)$. If one defines a filament as a dark elongated feature observable on the solar surface with a higher background brightness, then a given pixel x_{ij} may belong to a class of the filament elements, O_0, or the non-filament ones, O_1. Using the property that the influence of neighbouring pixels on the central pixel x_{ij} is restricted to k elements, one can define a rectangular window, a $k \times k$ matrix $\mathbf{P}^{(i,j)}$, with a central pixel x_{ij} and the $(kxk - 1)$ nearest neighbors; the window slides through the image matrix $\mathbf{X}$. A background of the filament elements is assumed to be additive to a pixel brightness that allows to evaluate and subtract it from the brightness values of the matrix $\mathbf{P}$. In order to do it one needs to define a background function $u = \varphi(\mathbf{X}; i, j)$, which is a contribution of background elements to the pixel x_{ij}. The parameters of this function can be learnt from the image data $\mathbf{X}$ by using ANNs. In order to do so, the training image data was created from a fragment with filament. The pixels in this data were manually labeled and assigned either to the class O_0 (filaments) and O_1 (background), which have a strong variation in brightness [1].

3. The Neural Network Technique for Filament Recognition

The idea behind the proposed method of filament recognition is to remove a contribution of the variable background elements represented by the function $u = \varphi(\mathbf{X}; s, l)$ learn from image data. One of the possible ways to define the function $\varphi(\mathbf{X}; s, l)$ is to approximate its values for each pixel x_{sl} of the given image data $\mathbf{X}$, $s = 1, \ldots, n$, $l = 1, \ldots, m$. With respect to filament recognition, one can use either a parabolic or linear approximation of this function; at the first instance, we used a linear approximation.

The algorithm is based on a standard sliding technique, for which the given image matrix $\mathbf{X}$ is transformed into a $\mathbf{z}^{(j)}$ column of the matrix $\mathbf{Z}$ consisting of $q = (n - k + 1)(m - k + 1)$ columns. Each column $\mathbf{z}^{(j)}$ presents the r pixels taken from the matrix $\mathbf{P}(k,k)$, where $r = k^2$ with $k = 3$ in this study. The matrix $\mathbf{P}$ slides one by one the pixels starting from the left upper corner s of the matrix X, so that the pixels (s,l) of X are placed in the column j of the matrix $\mathbf{Z}$ with a central pixel position defined as $i = (r + 1)/2$.

Now let us introduce a feed-forward ANN consisting of the two hidden and one output neurons as depicted in Fig 1. The first hidden neuron is fed by r elements of column vector $\mathbf{z}^{(j)}$. The second hidden neuron evaluates the value u_j of a background for the j-th column vector $\mathbf{z}^{(j)}$. The output neuron makes a decision, $y_i = (0,1)$, on the central pixel in the column vector $\mathbf{z}^{(j)}$.
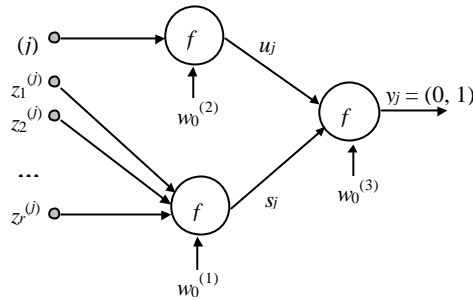
Fig 1. A feed-forward neural network with two hidden and one output neurons.

Assuming that the first hidden neuron is fed by r elements of the column vector $\mathbf{z}$, its output s is calculated as follows:

$$s_j = f(w_0^{(1)}, \mathbf{w}^{(1)}; \mathbf{z}^{(j)}), j = 1, \ldots, q, \tag{1}$$

where $w_0^{(1)}$, $\mathbf{w}^{(1)}$, and f are, respectively, the bias term, weighting vector and activation function of the neuron.

The activity of the second hidden neuron is proportional to the brightness of a background and can be described by the formula:

$$u_j = f(w_0^{(2)}, \mathbf{w}^{(2)}; j), j = 1, \ldots, q. \tag{2}$$

The bias term $w_0^{(2)}$ and weight vector $\mathbf{w}^{(2)}$ of this neuron are defined so as the output u is the evaluation of a background component contributed to the pixels of the jth column $\mathbf{z}^{(j)}$. These parameters are learnt from the image data $\mathbf{Z}$.

Taking into account the outputs of the hidden neurons, the output neuron makes a decision $y_j \in (0, 1)$ for each column vector $\mathbf{z}^{(j)}$ as follows:

$$y_j = f(w_0^{(3)}, \mathbf{w}^{(3)}; s_j, u_j), j = 1, \ldots, q. \tag{3}$$

Depending on activities of the hidden neurons, the output neuron assigns a central pixel of the column $\mathbf{z}^{(j)}$ either to the class O_0 or O_1.

4. Training the ANN

In order to train the feed-forward ANN plotted in Fig 1, one can use the back-propagation algorithms, which provide a global solution. These algorithms require to recalculate the output s_j for all q columns of the matrix $\mathbf{Z}$ and for each the training epochs. However, there are some local solutions, in which the hidden and output neurons are trained independently. As a result, the local solutions can be found much easer than the global ones while providing an acceptable accuracy of recognition.

The first algorithm is aimed to fit the weight vector of the second hidden, or a "background" neuron that evaluates a contribution of the background elements. An

example is depicted in Fig 2 where the top left plot shows the image matrix $\mathbf{X}$ presenting a filament on the unknown background and the top right plot reveals the corresponding filament elements depicted in black. The two bottom plots in Fig 2 show the outputs s (the left plot) and the weighted sum of s and u (the right one) plotted versus the columns of the matrix $\mathbf{Z}$. The right top plot shows the corresponding filament elements depicted in black. The bottom plots show the outputs s and the weighted sum of s and u, respectively, plotted versus the columns of the matrix $\mathbf{Z}$.

It can be seen from the left top plot that the brightness of a background varies from a lowest one in the left bottom corner to a highest one in the right top corner. Such variations of the background cause an increase of the output value u calculated over the q columns of the matrix $\mathbf{Z}$ (see the increasing curve depicted in the bottom left plot). This demonstrates that the background component is changed over $j = 1, \ldots, q$ much slower than the output s_j assuming the background component to be changed linearly with an increase of j.
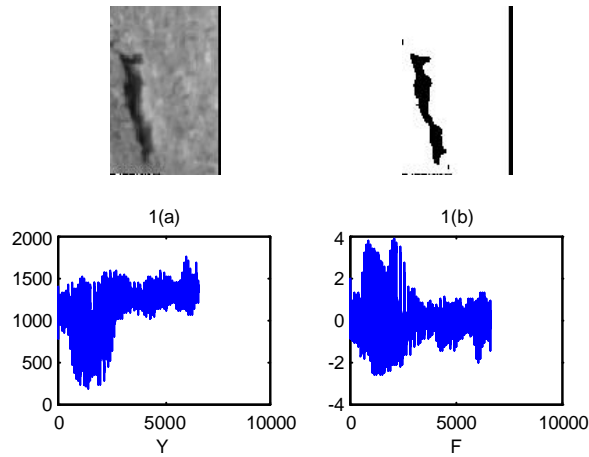

Fig 2: An example of the image matrix $\mathbf{X}$ depicting a filament on unknown background.

Based on this finding one can define a linear transform function of the "background" neuron as:

$$u_j = w_0^{(2)} + w_1^{(2)} j, j = 1, \ldots, q. \tag{4}$$

The weight coefficients $w_0^{(2)}$ and $w_1^{(2)}$ of this neuron can be fitted into the image data $\mathbf{Z}$ so that a squared error e between the outputs u_i and s_i is minimal:

$$e = \Sigma_j(u_j - s_j)^2 = \Sigma_i(w_0^{(2)} + w_1^{(2)} j - s_j)^2 \rightarrow min, j = 1, \ldots, q. \tag{5}$$

The weight coefficients can be found with the least deviation method, so the "background" neuron can be trained to evaluate the background component u. In the right bottom plot of Fig 2 there are presented the normalized values of s_i, which are no longer affected by the background component. The recognized filament elements are

shown at the right top plot in the Fig 2. By comparing the left and right top plots in Fig 2 one can reveal that the second hidden neuron has successfully learnt to evaluate a background component from the given image data $\mathbf{Z}$.

Before training the output neuron, the weights of a first hidden neuron are to be found. A local solution for this neuron is achieved for a set of the coefficients being equal to 1. For higher recognition accuracy one can update these weights by using the back-propagation algorithm.

After defining the weights for both hidden neurons, it is possible to train the output neuron, which makes the decisions between 0 or 1. Let us re-write the output y_i of this neuron as follows:

$$y_j = 0, \text{ if } w_1 s_j + w_2 u_j < w_0, \text{ and } y_j = 1, \text{ if } w_1 s_j + w_2 u_j \geq w_0. \tag{6}$$

Then the weight coefficients w_0, w_1, and w_2 can be fit in such way that the recognition error e is minimal:

$$e = \Sigma_i |y_i - t_i| \to min, \, i = 1, \ldots, h, \tag{7}$$

where $| \cdot |$ means a modulus operator, $t_i \in (0, 1)$ is the i-th element of a target vector $\mathbf{t}$ and h is the number of its components, namely, the training examples.

In order to minimize the error e one can apply any supervised learning methods, for example, the perceptron learning rule [5].

5. Results and Discussion

The neural network technique described above was applied for recognition of dark filaments in solar images. The full disk solar images obtained at the Meudon Observatory (France) during the period of March - April 2002 were used [1]. The fragments with filaments were picked from the images taken for various dates and regions on a solar disk with different brightness and inhomogeneity in the solar atmosphere. In total, there were 55 fragments selected depicting the filaments on a various background, one of them was used for training the ANN, the remaining 54 ones were used for testing the trained ANN.

The training error was 2.4% of 6936 pixels though the testing error was not calculated owing to the enormous labeling time required. However, by comparing the resultant and origin images visually (see Figures 2 and 3) it can be concluded that the algorithm recognised the testing filaments rather accurately. A further verification has been carried out from a comparison with the results obtained with the mosaic [3] and region growing [4] methods. The former was found to provide less accurate but faster results while the latter allowed identifying more details of filaments but required twice longer computation time.

A very interesting property of the algorithm is its ability to recognize the morphology of the multiplicative filaments depicted in the fragment (Figure 3). The original filaments are shown in the left plot and the recognized ones in the right plot. A visual comparison of the resulting and original images confirms that the proposed algorithm has recognized all four filaments rather close to their location and shape.
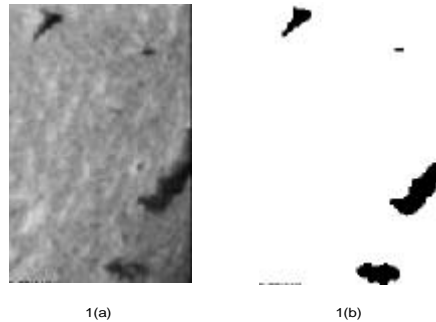
1(a)   1(b)

Fig 3: The recognition of the multiplicative filaments.

6. Conclusions

The automated recognition of filaments on the solar disk images is a difficult problem because of a variable background and inhomogeneities in the solar atmosphere. The proposed neural network technique can learn the recognition rules from a single image depicting the solar filament fragmented and labeled visually. The recognition rule has been successfully tested on the 54 other image fragments depicting filaments on different backgrounds. Despite the background differences, the trained neural network has properly recognized as single so multiple filaments presented in the testing image fragments. Therefore, the proposed neural network technique can be effectively used for an automated recognition of filaments in solar images.

References

1. V.V. Zharkova, S.S. Ipson, S.I. Zharkov, A. Benkhalil, J. Aboudarham, R.D. Bentley: A full disk image standardization of the synoptic solar observations at the Meudon Observatory, Solar Physics, (2003), accepted.
2. R.D. Bentley, et al: The European grid of solar observations, Proceedings of the 2nd Solar Cycle and Space Weather Euro-Conference, Vico Equense, Italy, 603, (2001).
3. R. Qahwaji, R. Green: Detection of closed regions in digital images. The International Journal of Computers and Their Applications, **8** (4), 202-207 (2001).
4. D.A. Bader, J. Jaja, D. Harwood, L.S., Davis: Parallel algorithms for image enhancement and segmentat ion by region growing with experimental study, The IEEE Proceedings of IPPS'96, 414 (1996).
5. C.M. Bishop: Neural networks for pattern recognition, Oxford University Press (1995).
6. I.T. Nabney: NETLAB: Algorithms for pattern recognition, Springer-Verlag (1995).